Ultrafast Ultrasound Imaging of Ocular Anatomy and Blood Flow

Raksha Urs,[1] Jeffrey A. Ketterling,[2] and Ronald H. Silverman[1,2]

[1]Department of Ophthalmology, Columbia University Medical Center, New York, New York, United States
[2]Frederic L. Lizzi Center for Biomedical Engineering, Riverside Research, New York, New York, United States

Correspondence: Raksha Urs, Harkness Eye Institute, Columbia University Medical Center, 635 W 165 Street, Room 711C, Box #42, New York, NY 10032, USA; ru2118@cumc.columbia.edu.

Submitted: March 10, 2016
Accepted: June 9, 2016

Citation: Urs R, Ketterling JA, Silverman RH. Ultrafast ultrasound imaging of ocular anatomy and blood flow. *Invest Ophthalmol Vis Sci.* 2016;57:3810–3816. DOI:10.1167/iovs.16-19538

Purpose. Ophthalmic ultrasound imaging is currently performed with mechanically scanned single-element probes. These probes have limited capabilities overall and lack the ability to image blood flow. Linear-array systems are able to detect blood flow, but these systems exceed ophthalmic acoustic intensity safety guidelines. Our aim was to implement and evaluate a new linear-array–based technology, compound coherent plane-wave ultrasound, which offers ultrafast imaging and depiction of blood flow at safe acoustic intensity levels.

Methods. We compared acoustic intensity generated by a 128-element, 18-MHz linear array operated in conventionally focused and plane-wave modes and characterized signal-to-noise ratio (SNR) and lateral resolution. We developed plane-wave B-mode, real-time color-flow, and high-resolution depiction of slow flow in postprocessed data collected continuously at a rate of 20,000 frames/s. We acquired in vivo images of the posterior pole of the eye by compounding plane-wave images acquired over $\pm 10^{\circ}$ and produced images depicting orbital and choroidal blood flow.

Results. With the array operated conventionally, Doppler modes exceeded Food and Drug Administration safety guidelines, but plane-wave modalities were well within guidelines. Plane-wave data allowed generation of high-quality compound B-mode images, with SNR increasing with the number of compounded frames. Real-time color-flow Doppler readily visualized orbital blood flow. Postprocessing of continuously acquired data blocks of 1.6-second duration allowed high-resolution depiction of orbital and choroidal flow over the cardiac cycle.

Conclusions. Newly developed high-frequency linear arrays in combination with plane-wave techniques present opportunities for the evaluation of ocular anatomy and blood flow, as well as visualization and analysis of other transient phenomena such as vessel wall motion over the cardiac cycle and saccade-induced vitreous motion.

Keywords: ultrafast ultrasound, choroid, optic nerve, blood flow

Numerous studies of retrobulbar hemodynamics have been carried out using color-flow and continuous-wave Doppler ultrasound. Particular interest now exists in the role of ocular blood flow in primary open-angle and normal-tension glaucoma.[1–8] Characterization of blood flow would also be of great clinical value for diagnosis and treating and monitoring conditions such as diabetic retinopathy,[9] macular degeneration,[10] myopia,[11] vascular occlusions,[12] malformations,[13] tumors,[14] and retinopathy of prematurity.[15] A serious impediment to clinical utilization of Doppler methods is the lack of access to linear-array ultrasound instrumentation in ophthalmic clinics. Current ophthalmic clinical systems rely on mechanically scanned, single-element, focused transducers, a technology that became obsolete in other clinical specialties decades ago. This situation exists for several reasons. Firstly, the U.S. Food and Drug Administration (FDA) 510k standards for ophthalmic exposure are more stringent than for any other clinical specialty.[16] Secondly, until recently, linear arrays could not provide the resolution required for ophthalmic diagnostic imaging due to challenges in fabrication of high-frequency (>10 MHz) arrays.

The emerging technology of compound coherent plane-wave imaging has the potential for imaging anatomy and blood flow at high sensitivity and low power. In conventional linear-array imaging, a subgroup of adjacent array elements (arrays typically consist of 64–256 transducer elements) emit a focused, converging wavefront by precisely timing the excitation of each subgroup element. The return echoes are then captured by the subgroup with a typical total round-trip time in the eye of approximately 0.1 ms. This process is then repeated, line by line, from one side of the array to the other to form a B-scan image. This iterative emit/capture process is time-consuming and reduces the potential maximum frame rate.

An alternative to this approach is plane-wave imaging, in which all array elements emit simultaneously (Fig. 1, center).[17] The incoherent addition of image frames acquired at different angles, or "compounding" (Fig. 1, right), for the purpose of improved signal-to-noise ratio (SNR), was first described in the early 1980s.[18] (The term "incoherent" refers to addition of enveloped B-mode images in which phase information is absent.) In 2009, Montaldo et al.[19] advanced the technique with coherent compounding.[19] (The term "coherent" refers to operation on phase-resolved echo data.) Data at each pixel

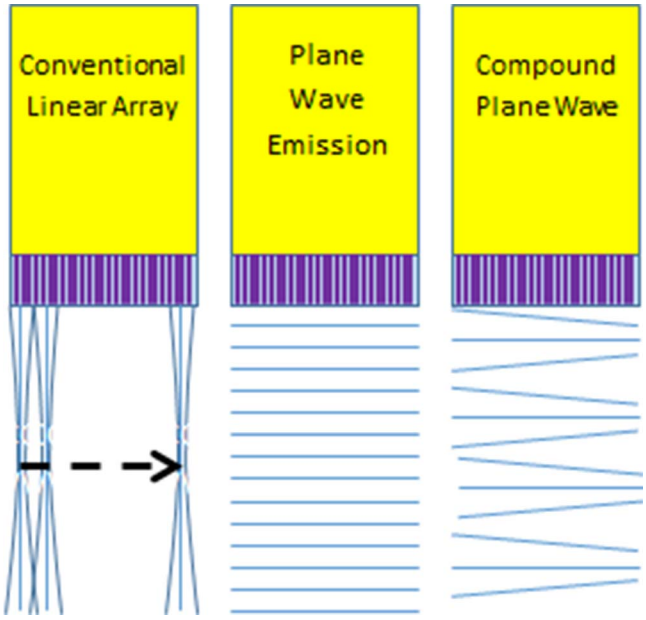

FIGURE 1. Schematic illustrating (*left*) conventional linear-array imaging, versus (*center*) plane-wave and (*right*) compound plane-wave imaging. In conventional linear-array imaging, groups of sequential array elements emit a focused beam with adequate time delay before excitation of the next group of elements to allow echo return. In plane-wave imaging, all elements emit simultaneously and B-mode images are formed at a rate comparable to the A-scan rate for the conventional array. Compounding involves emission of plane waves at a series of angles (only three angles shown here for illustrative purposes) and summation of echo data, resulting in improved image quality compared to simple plane-wave emission.

location acquired from emissions at different angles are added coherently, after beamforming, to obtain a final compound image. Because only a single plane-wave transmission is required to beamform the entire image, acquisition can be as much as two orders of magnitude faster than the conventional sequential linear-array pulse/echo approach and as much as three orders of magnitude faster than mechanically scanned single-element probes. This ultrafast modality is ideal for imaging of transient phenomena such as shear waves, elastic deformation, and blood flow.[20–23]

Another notable advantage of the plane-wave approach relevant to ophthalmic imaging is reduced ultrasound intensity, because there is no focusing on transmit.

This report will introduce the use of compound coherent plane-wave imaging for assessment of ocular anatomy and perfusion, which has heretofore not been demonstrated.

METHODS

All imaging was performed with a Verasonics Vantage 128 ultrasound engine (Verasonics, Inc., Kirkland, WA, USA). The Vantage 128 is a research platform that allows the user to program and control transmit and receive on each element of a linear array with user-developed MATLAB programs (The MathWorks, Inc., Natick, MA, USA). Phase-resolved echo data received by each transducer element are digitized at up to 62.5 MHz at 14 bits per sample.

All studies were performed with a 128-element, 18-MHz linear-array probe. The probe had an elevation aperture of 1.5 mm and was customized to provide an 18-mm focal depth in the elevation axis. Elements were spaced at 80-μm intervals along the azimuthal axis to provide an overall lateral dimension of approximately 1 cm. All images and acoustic intensity measurements were acquired at a 15-V excitation voltage.

Ultrasound Intensity Determination

We used a calibrated needle hydrophone (Precision Acoustics, Inc., Dorset, UK) with 40-μm-diameter sensor to measure the acoustic pressure at and around the probe's elevation focus in plane-wave and conventionally focused modes, where a relatively weak focal ratio of f4 was used. (Typically, f-ratios between 1.5 and 4 are used for B-mode imaging with linear arrays.) We used a two-cycle excitation to simulate B-mode and a four-cycle excitation to simulate color-flow Doppler mode.

Resolution and SNR

We acquired compound coherent plane-wave images of a 0.02-mm-diameter polypropylene surgical thread (model no. 8065-307601; Alcon Laboratories, Inc., Fort Worth, TX, USA) coherently compounding 1, 3, 5, 10, or 50 transmissions acquired at equally spaced angular intervals over ±10°. An 18-MHz, two-cycle waveform was used for excitation. We acquired 14 images per imaging condition, from which we determined the SNR (from signal maximum divided by root mean squared background noise) and the 12-dB lateral beamwidth.

Ultrafast B-Mode Imaging

Images of the posterior pole were acquired from 1, 3, 5, 10, and 50 successive angles over a ±10° range at pulse repetition frequency (PRF) of 10 kHz, so that coherent compound images were formed at 10/n kHz, where n is the number of angles. Coherent compound images of the eye were acquired for each value of n and were evaluated qualitatively. Images of the whole eye were acquired by compounding 20 successive angles and compared with images of the same eye acquired with a 10-MHz single-element, mechanically scanned ophthalmic ultrasound system (Aviso; Quantel Medical, Bozeman, MT, USA).

Flash Doppler Imaging

We implemented flash Doppler[24] for real-time depiction of blood flow in the context of B-mode images In this mode, two-cycle plane waves were emitted at equally spaced angles over ±10° to form B-mode images in real time. At 8.2-ms intervals, B-mode acquisition was interrupted and a series of 28 four-cycle plane waves were emitted at a single 12° angle at a 4-kHz PRF. Doppler analysis was then performed at each pixel position, and color-flow data depicting velocity or power were superimposed upon the grayscale B-mode image in real time.

Plane-Wave Doppler Imaging

We developed software to allow high-speed data acquisition followed by postprocessing for high-resolution depiction of slow flow. We acquired three coherent plane-wave images over an angle of ±10° at a 20-kHz PRF (6666 coherently compounded images per second) for 1.6 seconds. We postprocessed data with custom software developed in MATLAB, using techniques similar to those described in reports by Mace et al.[25] and Demene et al.[26] In brief, we used a singular value decomposition (SVD) spatiotemporal filter[27] to suppress clutter signals originating from stationary and slowly moving tissue while retaining signals from moving blood cells. We then summed the intensities from the blood signal to produce a high-quality power Doppler image. By using a sliding

Table 1. Measurements of Acoustic Intensity Parameters for the Conventional and Plane-Wave Imaging Techniques Compared to FDA 510k Ophthalmic Safety Limits

Mode	Frames per Second	$I_{SPPA.3}$ W/cm^2	$I_{SPTA.3}$ mW/cm^2	MI
Focused	25	22.1	0.5	0.21
Conventional Doppler	25	35.9	2.1	0.32
Plane-wave Doppler	20,000	3.0	7.0	0.07
Flash Doppler	318	6.5	0.6	0.13
Ophthalmic FDA 510k limit		28.0	17.0	0.23

$I_{SPPA.3}$, derated spatial peak pulse average intensity; $I_{SPTA.3}$, derated spatial peak temporal average intensity; MI, mechanical index.

analysis window of 76.8-ms duration and a step size of 4.8 ms (72-ms overlap between successive analyses), we produced a temporal series of images demonstrating flow variation over the 1.6-second period of data acquisition, which was sufficiently long to capture two cardiac cycles. We used the frequency information of this temporal series to plot spectrograms representing the simultaneous flow speed at various locations as a function of time.

Our software allowed B-mode imaging with or without real-time, flash color-flow Doppler, allowing identification of anatomy and regions where flow was present. The user could at any time interrupt real-time imaging to acquire a block of up to 1.6 seconds of plane-wave data for postprocessing to produce high-resolution color-flow power Doppler image sequences.

Clinical Imaging Setup

The study followed the principles of the Declaration of Helsinki, and the research procedure was approved by the Institutional Review Board (IRB)/Ethics Committee. After obtaining informed consent, imaging was performed by placing the horizontally oriented probe in contact with the lower eyelid after application of coupling gel (GenTeal; Alcon Laboratories, Inc.) on the probe surface. The subject was scanned in a seated position with the eye in a forward or slightly upward direction of gaze, with both eyes open. Data were acquired in a plane encompassing and extending temporal to the optic disc, capturing the optic nerve head (ONH) and macula region. Plane-wave B-mode, flash Doppler, and 1.6-second blocks of plane-wave data for depiction of vascular flow were acquired. In order to perform repeatability measurements, four sets of data from the same location were acquired and processed and, from the spectrograms, the peak systolic velocity (PSV) and the end diastolic velocity (EDV) were measured in the short posterior ciliary artery (SPCA) at a position prior to the branching into distal SPCAs. Resistive index (RI) was calculated as RI = (PSV − EDV)/PSV.

Results

Ultrasound Intensity Determination

Table 1 shows measurements of acoustic intensity in conventional and plane-wave modes in relation to FDA 510k maximum allowable levels.[9] Results show the plane-wave Doppler mode to have significantly lower instantaneous and temporally averaged intensities and mechanical index than the conventionally focused mode. This is particularly the case with pulsed Doppler, where in the conventionally focused mode, instantaneous intensity exceeded FDA limits even with weak f4 focusing. Plane-wave intensities in all modes are well below the FDA limits.

Table 2. Signal-to-Noise Ratio (SNR) and 12-dB Lateral Beamwidth, Mean ± Standard Deviation, of Point Spread Function Calculated From Coherent Compound Plane-Wave Images of a 20-μm Diameter Polypropylene Thread Produced From *N* Subimages Acquired at Equal Angular Increments Over ±10° Range

N Angles	SNR, dB	Beamwidth, mm
1	57.8	0.52 ± 0.0009
3	63.9	0.42 ± 0.0007
5	66.1	0.26 ± 0.0002
10	68.4	0.27 ± 0.0007
50	76.1	0.27 ± 0.0038

Resolution and SNR

Table 2 shows the SNR and 12-dB beam width of the point spread function for coherent compound images formed with 1, 3, 5, 10, and 50 angled plane-wave images. There was significant improvement in SNR as the number of coherent additions increased. Lateral resolution was the worst for $n = 1$, because no angle compounding takes place under this condition. Resolution improved with compounding, but was relatively unchanged as the number of coherent additions was increased. This is expected because lateral resolution is dependent only on the maximum angle range of ±10°, which is held constant for $n > 1$.

Ultrafast B-Mode Imaging

Figure 2 shows compound coherent plane-wave images of the ONH region obtained using 1, 3, 5, 10, and 50 plane-wave transmissions acquired over a ±10° angle at a PRF of 10 kHz. An improvement in SNR was evident as the number of plane-wave images per compound image was increased.

Figure 3 shows B-mode images of a human eye obtained with a conventional 10-MHz, single-element, mechanically scanned transducer and with the 18-MHz linear array. The linear-array image was generated by coherent compounding of 20 angled plane waves over a ±10° range. Plane-wave images provided superior sensitivity, demonstrating vitreous inhomogeneities and improved anatomic depiction of the anterior segment, including the anterior chamber and cornea. The detached posterior vitreous face appeared brighter using the single-element probe, possibly due to its scan geometry and axially symmetric focus.

Flash Doppler Imaging

Figure 4 shows real-time power and velocity Doppler images of the ONH region obtained with a 4-kHz Doppler PRF. We found detection of blood flow in the region of the ONH (central retinal artery and short posterior ciliary arteries) and choroid to be easily accomplished. At a PRF of 4 kHz, aliasing will occur for axial velocities above 8.5 cm/s.

Plane-Wave Doppler Imaging

Figure 5 shows compound plane-wave and power Doppler images of the ONH region obtained from two sets of data. The figures clearly depict choroidal perfusion over the entire region being imaged and also flow in the central retinal artery and short posterior ciliary arteries. At a 6.66-kHz PRF, aliasing will occur at axial velocities above 14 cm/s. Choroidal flow velocities, however, are slower than this, and power Doppler

Investigative Ophthalmology & Visual Science

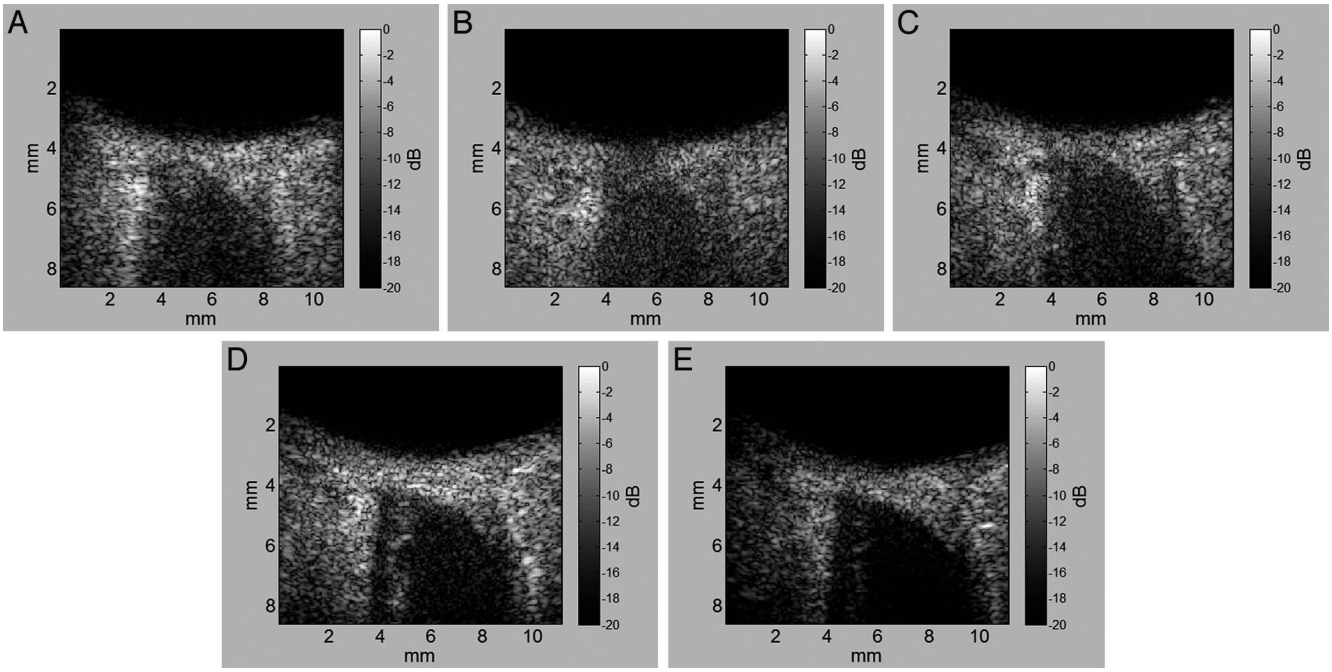

Figure 2. Compound plane-wave images of the optic nerve head region of a 66-year-old male subject obtained with (**A**) 1, (**B**) 3, (**C**) 5, (**D**) 10, and (**E**) 50 plane-wave images coherently added to form the final image.

is in any case unaffected by aliasing. A temporal series of images obtained from the sliding window analysis demonstrates flow variation over the cardiac cycle (Supplementary Movie Clip S1). Figure 6 shows flow-speed variation as a function of time in the choroid, central retinal vein (CRV), SPCA, and distal SPCA. Results show aliasing in the distal SPCA where the speed is greater than 14 cm/s. Table 3 summarizes repeatability of flow measurements of the SPCA over four scan sets of one subject.

Discussion

In this report, we demonstrate ultrahigh-speed ultrasound imaging of the eye at a frame rate of up to 20,000 Hz. As each image consists of 128 vectors (i.e., A-scans), the maximum imaging speed may be expressed as 2.56 MHz in A-scans/s, comparable to the speed of advanced ultrahigh-speed swept-source optical coherence tomography (OCT) systems.[28,29] Indeed, there are many methodologic parallels between the ultrasound methods described in this report and OCT

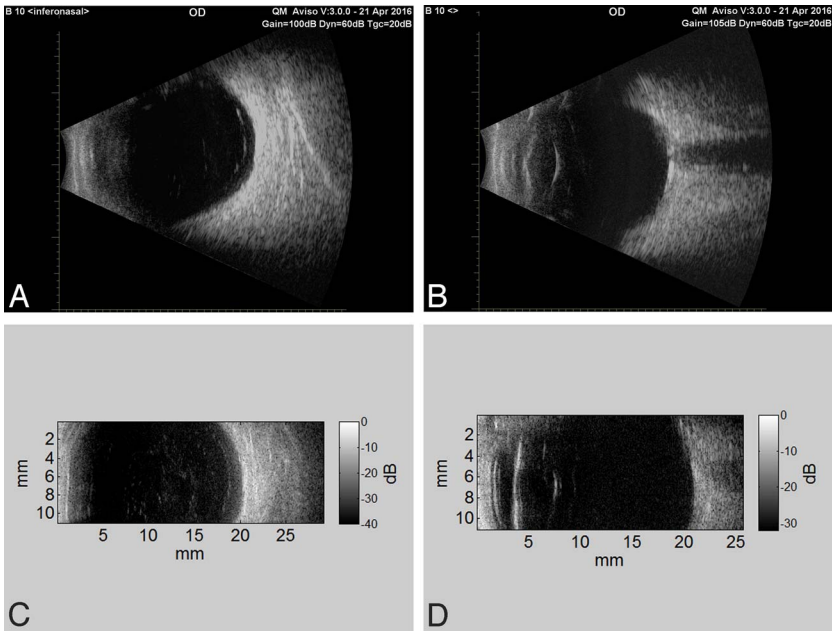

Figure 3. Comparative B-mode images of a 66-year-old male subject obtained with an ophthalmic B-scanner using a 10-MHz single-element probe (**A**, **B**) versus the 18-MHz linear array by coherent compounding of 20 angled plane-wave images over a ±10° range (**C**, **D**).

Investigative Ophthalmology & Visual Science

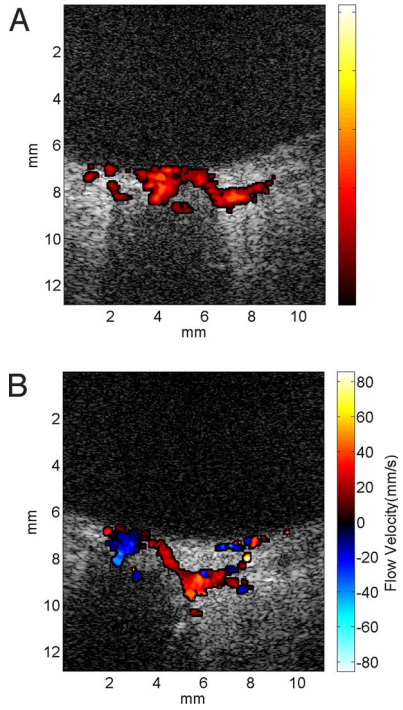

FIGURE 4. Real-time (**A**) power Doppler and (**B**) velocity Doppler images of the posterior pole region of a 66-year-old male subject obtained with a 4-kHz Doppler PRF using the flash Doppler technique. B-mode grayscale images were generated by coherent compounding of seven angled plane-wave images over a ±10° range.

angiography,[30] which, like plane-wave ultrasound, requires high-speed acquisition of successive B-scans to demonstrate flow. While the superior resolution attainable by OCT makes it the optimal modality for imaging of the retina, the better penetration of ultrasound is advantageous for evaluation of optically occult anatomy and pathologies, including the orbit, choroid, ciliary body, tumors, and saccade-induced vitreous motion.

We have described two methods for imaging of blood flow. The first method is a real-time method that interleaves compound plane-wave depiction of anatomy with color-flow Doppler derived from multicycle plane-wave transmissions emitted from a single angle. Because color-flow Doppler utilizes a narrowband emission from just a single transmit angle, color-flow resolution is dependent on the angle of plane-wave transmission and does not benefit from the improved SNR and lateral resolution of multiangle compounding. The second method involves postprocessing of blocks of multi-angle plane-wave data acquired continuously for greater than 1 second. This method is particularly useful for depiction of slow flow, and it offers improved spatial resolution and SNR because of the multiangle compounding. One drawback of the compounding approach is that several gigabytes of data need to be acquired and the current MATLAB-based postprocessing for production of blood flow images requires approximately 15 minutes to complete. This time could be sped up significantly with the use of graphics processing units and algorithm optimization.

In compound coherent plane-wave imaging, there is no tradeoff between frame rate and the size of the color-flow box because the entire medium is insonified with each transmission. Flow velocity estimation is obtained simultaneously for all image pixels, leading to full two-dimensional Doppler flow imaging. Power Doppler is advantageous in situations of slow flow in small tortuous vessels such as in the choroid. Power Doppler encodes an estimate of the integrated Doppler power spectrum rather than frequency shift (which encodes velocity), so that power Doppler intensity at each pixel position is a function of the amount of moving blood at that location.[31,32] High-resolution, power-Doppler depiction of choroidal flow may thus offer a means for quantitative study of choroidal

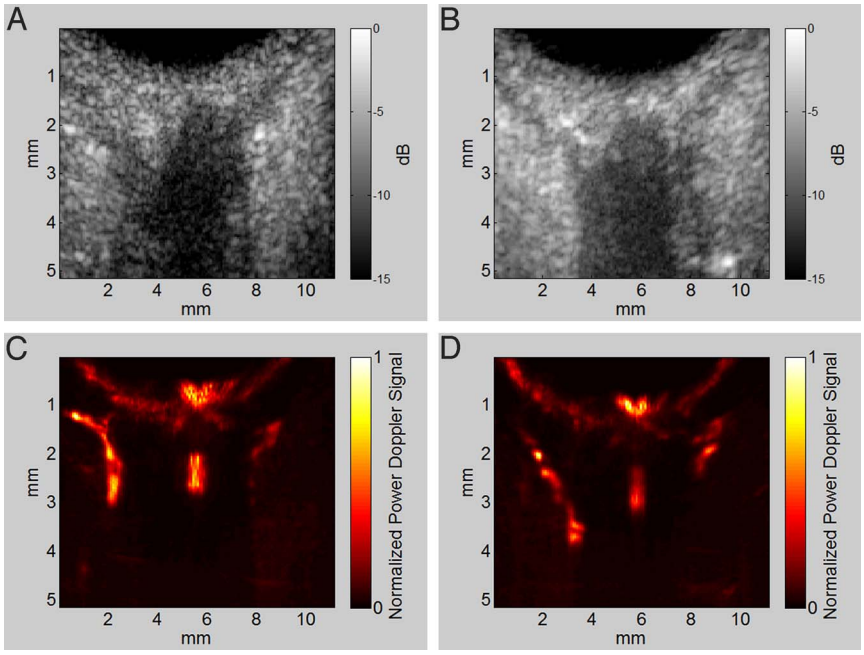

FIGURE 5. Average compound plane-wave images (**A**, **B**), and power Doppler images (**C**, **D**) of the ONH region obtained from two sets of data from a healthy 46-year-old female subject. Each set was acquired for 1.6 seconds at 6.66-KHz compound imaging frame rate (three angles over ±10° per image). After postprocessing with the plane-wave Doppler technique, choroidal perfusion and flow in the short posterior ciliary artery and central retinal vein are visualized.

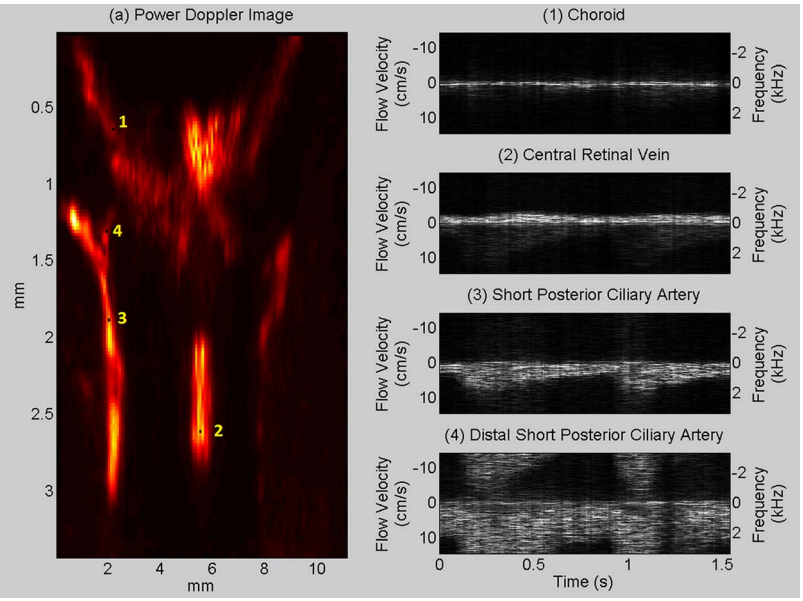

Figure 6. Spectrograms of (1) choroid, (2) central retinal vein (3), short posterior ciliary artery, and (4) distal short posterior ciliary artery depict flow velocity variation as a function of time. Aliasing is evident in the distal short posterior ciliary artery where the flow speed is higher than 14 cm/s.

perfusion. Another advantage of this method is that it allows a spectral and temporal description of blood flow at any position over the whole image at any time point.

We showed that this technology can be used for the depiction and quantification of blood flow over a cardiac cycle in the orbital vessels and choroid. The 6.66-kHz PRF (of the compound image sequence) we used for flow imaging was a good compromise between the detection of slow flow in the choroid and the depiction of high velocities in the central retinal vein and short posterior ciliary arteries (albeit with aliasing). Working at a PRF of 20 kHz (one angle), velocities up to 42 cm/s can be captured without aliasing, although resolution will be reduced. A lower PRF, on the other hand, would increase sensitivity to slow flow. The choice of an 18-MHz probe was based on a tradeoff between resolution and attenuation, both of which increase with frequency. At 18 MHz, an axial resolution of approximately 80 μm was obtained, and image quality was good to a tissue depth of at least 6 mm beyond the retina. The methods described in this paper can readily be implemented using lower frequencies, which would enable visualization of retrobulbar flow to the orbital apex. Lower frequencies would also allow higher flow rates to be detected before encountering aliasing, but would degrade resolution. Conversely, higher frequencies would enable improved resolution and allow for imaging of flow in the anterior segment.

We demonstrated how the compounding process provides a substantial increase in SNR. Increased SNR, combined with ultrafast real-time imaging, would be particularly useful for visualization of faint reflectors within the vitreous ("floaters") during voluntary saccades to evaluate organization and possible vitreoretinal traction. Also, the presence of vitreous floaters has been shown to correlate with contrast sensitivity.[33]

Table 3. Mean, Standard Deviation, and Coefficient of Variation of the Peak Systolic Velocity, End Diastolic Velocity, and Resistive Index of the Short Posterior Ciliary Artery Calculated From Four Scans of One Eye

SPCA Measurements	Mean	Standard Deviation	Coefficient of Variation
PSV, cm/s	8.28	0.20	2.41%
EDV, cm/s	3.40	0.43	12.70%
RI	0.59	0.05	7.78%

While the emphasis of this report is on B-mode and blood flow imaging using the plane-wave technique, this method can also capture other transient motions. Rossi et al.,[34] for instance, studied saccade-induced vitreous velocity fields as a potential means for assessing risk of retinal tears. They used a 20-MHz mechanically scanned transducer acquiring 20 images per second, which could be dramatically improved upon by plane-wave methods. Tanter et al.[35] described use of plane waves to capture shear waves to characterize elasticity in ex vivo enucleated porcine corneas, and Toubol et al.[36] used this technique to evaluate cross-linked corneas of rabbits. Ultrafast imaging might also allow assessment of vessel wall motions over the cardiac cycle, providing information about vessel wall rigidity. The ultrahigh-speed technique could also be invaluable for study of ex vivo ocular deformation in blunt force trauma.

Most significantly in terms of clinical application, plane-wave technology produces far lower acoustic intensity than conventionally scanned arrays, which will allow FDA-compliant instrumentation for ocular blood flow imaging.

While plane-wave array technology is certainly more complex than single-element mechanical B-scanners, given its benefits in speed, blood flow depiction, and safety, we can reasonably expect that commercial systems can be manufactured at prices comparable to OCT systems, making clinical translation a feasible prospect. The introduction of this technology into ophthalmology will open a new avenue toward investigation of hemodynamics in glaucoma and other ocular pathologies.

Acknowledgments

Supported by National Institutes of Health Grants EY025215 and P30 EY019007 and an unrestricted grant to the Department of Ophthalmology of Columbia University from Research to Prevent Blindness.

Disclosure: **R. Urs**, None; **J.A. Ketterling**, None; **R.H. Silverman**, None

References

1. Asejczyk-Widlicka M, Krzyzanowska-Berkowska P, Sander BP, Iskander DR. Age-related changes in ocular blood velocity in suspects with glaucomatous optic disc appearance. Comparison with healthy subjects and glaucoma patients. *PLoS One*. 2015;10:e0134357.
2. Findl O, Strenn K, Wolzt M, et al. Effects of changes in intraocular pressure on human ocular haemodynamics. *Curr Eye Res*. 1997;16:1024–1029.
3. Joos KM, Kay MD, Pillunat LE, et al. Effect of acute intraocular pressure changes on short posterior ciliary artery haemodynamics. *Br J Ophthalmol*. 1999;83:33–38.
4. Michelson G, Langhans MJ, Harazny J, Dichtl A. Visual field defect and perfusion of the juxtapapillary retina and the neuroretinal rim area in primary open angle glaucoma. *Graefes Arch Clin Exp Ophthalmol*. 1998;236:80–85.
5. Rojana Pongpun P, Drance SM, Morrison BJ. Ophthalmic artery flow velocity in glaucomatous and normal subjects. *Br J Ophthalmol*. 1993;77:25–29.
6. Plange N, Kaup M, Weber A, et al. Performance of colour Doppler imaging discriminating normal tension glaucoma from healthy eyes. *Eye*. 2009;23:164–170.
7. Stalmans I, Harris A, Fieuws S, et al. Color Doppler imaging and ocular pulse amplitude in glaucomatous and healthy eyes. *Eur J Ophthalmol*. 2009;19:580–587.
8. Abegao Pinto L, Vandewalle E, Stalmans I. Disturbed correlation between arterial resistance and pulsatility in glaucoma patients. *Acta Ophthalmol*. 2012;90:214–220.
9. Goh JK, Cheung CY, Sim SS, et al. Retinal imaging techniques for diabetic retinopathy screening. *J Diabetes Sci Technol*. 2016;10:282–294.
10. Burgansky-Eliash Z, Barash H, Nelson D, et al. Retinal blood flow velocity in patients with age-related macular degeneration. *Curr Eye Res*. 2014;39:304–311.
11. Yang YS, Koh JW. Choroidal blood flow change in eyes with high myopia. *Korean J Ophthalmol*. 2015;29:309–314.
12. Jaulim A, Ahmed B, Khanam T, Chatziralli IP. Branch retinal vein occlusion: epidemiology, pathogenesis, risk factors, clinical features, diagnosis, and complications. An update of the literature. *Retina*. 2013;33:901–910.
13. Warrier S, Prabhakaran VC, Valenzuela A, et al. Orbital arteriovenous malformations. *Arch Ophthalmol*. 2008;126:1669–1675.
14. Iveković R, Lovrencić-Huzjan A, Mandić Z, Talan-Hranilović J. Color Doppler flow imaging of ocular tumors. *Croat Med J*. 2000;41:72–75.
15. Hartenstein S, Müller B, Metze B, Czernik C, Bührer C. Blood flow assessed by color Doppler imaging in retinopathy of prematurity. *J Perinatol*. 2015;35:745–747.
16. Food and Drug Administration. *Information for Manufacturers Seeking Marketing Clearance of Diagnostic Ultrasound Systems and Transducers*. Rockville, MD: Center for Devices and Radiological Health, Food and Drug Administration, US Department of Health and Human Services; 2008:19.
17. Tanter M, Fink M. Ultrafast imaging in biomedical ultrasound. *IEEE Trans Ultrason Ferroelectr Freq Control*. 2014;61:102–119.
18. Berson M, Roncin A, Pourcelot L. Compound scanning with an electrically steered beam. *Ultrason Imaging*. 1981;3:303–308.
19. Montaldo G, Tanter M, Bercoff J, et al. Coherent plane-wave compounding for very high frame rate ultrasonography and transient elastography. *IEEE Trans Ultrason Ferroelectr Freq Control*. 2009;56:489–506.
20. Tanter M, Bercoff J, Sandrin L, Fink M. Ultrafast compound imaging for 2-D motion vector estimation: application to transient elastography. *IEEE Trans Ultrason Ferroelectr Freq Control*. 2002;49:1363–1374.
21. Tanter M, Bercoff J, Athanasiou A, et al. Quantitative assessment of breast lesion viscoelasticity: initial clinical results using supersonic shear imaging. *Ultrasound Med Biol*. 2008;34:1373–1386.
22. Bercoff J, Montaldo G, Loupas T, et al. Ultrafast compound Doppler imaging: providing full blood flow characterization. *IEEE Trans Ultrason Ferroelectr Freq Control*. 2011;58:134–147.
23. Ekroll IK, Swillens A, Segers P, et al. Simultaneous quantification of flow and tissue velocities based on multi-angle plane wave imaging. *IEEE Trans Ultrason Ferroelectr Freq Control*. 2013;60:727–738.
24. Flynn J, Daigle R, Pflugrath L, Kaczkowski P. High frame rate vector velocity blood flow imaging using a single plane wave transmission angle. *Proc IEEE Int Ultrason Symp*. 2012;323–325.
25. Mace E, Montaldo G, Osmanski B, et al. Functional ultrasound imaging of the brain: theory and basic principles. *IEEE Trans Ultrason Ferroelectr Freq Control*. 2013;60:492–506.
26. Demene C, Pernot M, Biran V, et al. Ultrafast Doppler reveals the mapping of cerebral vascular resistivity in neonates. *J Cereb Blood Flow Metab*. 2014;34:1009–1017.
27. Demene C, Deffieux T, Pernot M, et al. Spatiotemporal clutter filtering of ultrafast ultrasound data highly increases Doppler and fUltrasound sensitivity. *IEEE Trans Med Imaging*. 2015;34:2271–2285.
28. Choi W, Moult EM, Waheed NK, et al. Ultrahigh-speed, swept-source optical coherence tomography angiography in nonexudative age-related macular degeneration with geographic atrophy. *Ophthalmology*. 2015;122:2532–2544.
29. Choi W, Potsaid B, Jayaraman V, et al. Phase-sensitive swept-source optical coherence tomography imaging of the human retina with a vertical cavity surface-emitting laser light source. *Opt Lett*. 2013;38:338–340.
30. Makita S, Hong Y, Yamanari M, et al. Optical coherence angiography. *Opt Express*. 2006;14:7821–7840.
31. Rubin JM, Bude RO, Carson PL, et al. Power Doppler US: a potentially useful alternative to mean frequency-based color Doppler US. *Radiology*. 1994;190:853–856.
32. Rubin JM, Adler RS, Fowlkes JB, et al. Fractional moving blood volume: estimation with power Doppler US. *Radiology*. 1995;197:183–190.
33. Mamou J, Wa CA, Yee KM, et al. Ultrasound-based quantification of vitreous floaters correlates with contrast sensitivity and quality of life. *Invest Ophthalmol Vis Sci*. 2015;56:1611–1617.
34. Rossi T, Querzoli G, Pasqualitto G, et al. Ultrasound imaging velocimetry of the human vitreous. *Exp Eye Res*. 2012;99:98–104.
35. Tanter M, Touboul D, Gennisson JL, et al. High-resolution quantitative imaging of cornea elasticity using supersonic shear imaging. *IEEE Trans Med Imaging*. 2009;28:1881–1893.
36. Touboul D, Gennisson JL, Nguyen TM, et al. Supersonic shear wave elastography for the in vivo evaluation of transepithelial corneal collagen cross-linking. *Invest Ophthalmol Vis Sci*. 2014;55(3):1976–1984.